Crosstalk analysis and optimization in a compact microwave-microfluidic device towards simultaneous sensing and heating of individual droplets

OPEN ACCESS
IOP Publishing
Journal of Micromechanics and Microengineering
J. Micromech. Microeng. **32** (2022) 095005 (10pp)
https://doi.org/10.1088/1361-6439/ac821e

Crosstalk analysis and optimization in a compact microwave-microfluidic device towards simultaneous sensing and heating of individual droplets

Weijia Cui[1], **Zahra Abbasi**[2] **and Carolyn L Ren**[1,*]

[1] Department of Mechanical and Mechatronics Engineering, University of Waterloo, Waterloo, ON, Canada
[2] Department of Electrical and Software Engineering, University of Calgary, Calgary, AB, Canada

E-mail: c3ren@uwaterloo.ca

Received 5 October 2021, revised 10 June 2022
Accepted for publication 18 July 2022
Published 4 August 2022

Abstract

Non-invasive contactless simultaneous sensing and heating of individual droplets would allow droplet microfluidics to empower a wide range of applications. However, it is challenging to realize simultaneous sensing and heating of individual droplets as the resonance frequency of the droplet fluid, which is decided by its permittivity, must be known so that energy is only supplied at this frequency for droplet heating with one resonator. To tailor the energy transfer in real-life heating applications, the droplet has to be sensed first to identify its corresponding resonance frequency, which is used to dynamically tune the frequency for supplying the required energy for heating this particular droplet. To achieve this goal, two resonators are needed, with one for sensing and one for heating. Integrating multiple resonators into one typical microfluidic device limits placement of the resonators to be as close as possible, which would raise the concern of crosstalk between them. The crosstalk would result in inaccurate sensing and heating. This study focuses on numerically and experimentally investigating the effect of influencing parameters on the crosstalk between two adjacent resonators with the ultimate goal of providing guidance for multiplexing the resonators in a typical microfluidic device. ANSYS HFSS is used to perform the electromagnetic analysis based on the finite element method. Experimental studies are conducted on a microfluidic chip integrated with two resonators to validate the numerical results. An optimal distance between two resonators is suggested, with the recommendation for the resonator size and heating power towards simultaneous sensing and heating of individual droplets.

* Author to whom any correspondence should be addressed.

Supplementary material for this article is available online

Keywords: microfluidics, microwave sensing, microwave heating, lab-on-chip, microwave resonators

(Some figures may appear in colour only in the online journal)

1. Introduction

By integrating a series of functions onto one single platform, lab-on-chip (LOC) devices present several advantages over their traditional counterparts, such as reduced sample consumption, shortened analysis time, lower cost, and higher efficiency [1]. Recently, the development of droplet microfluidic systems has offered a practical solution to improve and study the dynamics of many chemical and biochemical reactions, facilitating the development of LOC [2]. Further reduced sample consumption, increased reaction rate, and isolation of individual droplets by their carrier fluids make droplet microfluidic systems a strong candidate to serve as reactors/detectors, complementing or replacing their conventional counterparts [3]. Integrating droplet microfluidics functions into LOC platforms offers tremendous potential to make typical reactors such as polymerase chain reaction process [4] or detection methods [5], suitable for point-of-care (POC) applications [6, 7]. However, some challenges remain related to the applicability of droplet microfluidic systems on a large scale, which lies in both fabrication techniques and the ability to accommodate multiple functional units in a limited space without compromising their performance. In addition to droplet manipulations such as droplet generation, splitting and merging, droplet sensing and heating are the key functions to be integrated for chemical and biochemical applications [8].

Sensing in droplet microfluidics devices provides detailed information regarding materials' contents, concentration, size, and temperature, which is essential to fully realize the potential of droplet microfluidics. Optical methods that are commonly used in microfluidic systems [9] provide information about different materials by analyzing the light source changes from fluorescent, infrared, or UV [10]. These methods often require relatively bulky detection systems, tend to exhaust the image analysis processor, or involve fluorescent labeling, limiting their applications for POC. Electrical methods are alternative for sensing in microfluidics in favor of POC applications [11]. Capacitive sensors, electrochemical sensors, and impedance variation-based detection methods are widely available to extract material information by monitoring and processing the variation in the output electrical signals. Leveraging electrical techniques to detect droplet size and flow rate, or general control over and handling droplet manipulation, has been reported in the literature [12, 13]. However, detecting materials that are not electroactive or detecting droplets at high throughput rates [14] remain challenging for conventional electrical methods.

Planar microwave resonators have recently attracted a lot of attention from academia and industry for sensing applications due to their simple fabrication process, easy integration with complementary metal-oxide semiconductor (CMOS), LOC compatibility, and flexibility in design [15]. In microwave sensing, detection is carried out by utilizing the interaction between the electromagnetic (EM) field around the microwave sensor with the sensing material in the surrounding environment, which empowers them to perform highly accurate non-contact and real-time sensing and detection while materials under the test changes in electrical properties (dielectric permittivity or conductivity). Their exceptional performance in non-contact and distant sensing is desired for microfluidics since the need for chemical modification or physical contact with the sample under the test is eliminated [14, 16, 17]. Their applications for exploring the dielectric properties of materials, especially liquid materials [18], hazardous gas concentration monitoring [19, 20], biomedical detection [21], and chemical solutions sensing [22–24] have also been demonstrated. It is promising to leverage their sensing potential for droplet microfluidic applications.

Heating in a microfluidic platform is desired for many applications, such as DNA amplification [25] and materials synthesis [26]. In microfluidics, available popular heating approaches rely on heat conduction using one of the resistant heating, Peltier, and Joule heating methods, where simple elements are used to realize efficient heating [27]. However, these heating techniques suffer from imprecise heating, which is a severe drawback of localized heat production desired for heating individual droplets. Optical methods such as laser heating have also been used due to their efficient and precise heat production but relying on expensive equipment, and tedious alignment limits their broad application. As a result, portable, efficient, and low-cost heating methods are desired to be integrated with microfluidic systems for multiple applications.

The application of planar microwave structures in microfluidic systems has been demonstrated for localized heating [28]. In the microwave frequency range, some liquid materials have the ability to convert EM energy to heat due to molecular friction. This kind of heating is volumetric and spontaneous in nature, which means that the heating can be self-triggered by materials entering the microwave heater region [29]. Using microwave-based heating structures can directly provide power to the target materials and realize fast heating, significantly reducing reaction time for many applications [30]. These advantages make microwave technology an excellent candidate to be integrated with microfluidic systems for both sensing and heating of individual droplets.

The main element of the proposed microwave system for sensing and heating is a split-ring resonator (SRR). The SRR is able to distinguish materials by their different electrical properties such as permittivity and conductivity. The changes in these properties cause variations in the system's frequency response, which can be used for sensing purposes.

Additionally, delivering microwave power to the sensing region of the SRR limits the power to be received only by the droplet passing the resonator, leaving the surrounding media unaffected. Microwave sensing and heating of individual droplets have been demonstrated separately with a single SRR [31, 32]; however, its promise for simultaneous sensing and heating of droplets has not been realized, which requires more than one SRR to be integrated.

Selectively heating of individual droplets to the desired temperature is very challenging. It needs to acquire the droplet content information by sensing first, which is then used as the feedback to tune the power delivery at this frequency for selectively heating this particular droplet. Two resonators are needed to realize this procedure, with one for sensing and the other for heating, and they need to work together and be controlled by a backstage system. Integrating two or more microwave resonators into a typical microfluidic chip of $1'' \times 3''$ presents the potential to realize simultaneous microwave sensing and heating. For multiplexing purposes, for example, integrating multiple SRRs into one chip, the resonators should be placed as close as possible, which however would raise the concern of crosstalk between the resonators. The crosstalk here is referred to the phenomenon that one signal creates the undesired signal in another circuit generating inaccurate results. This study presents a detailed analysis of the influencing design and operation parameters of the two SRRs on the crosstalk between them towards simultaneous sensing and heating of droplets. The SRRs are a copper trace that offers consistent performance, making the proposed structure highly reliable. This brief will be continued in section 2 with a focus on methodology, and the simulations and measurement results for different studies are presented in section 3, followed by a conclusion in section 4.

2. Methodology

2.1. Effect of design parameters on crosstalk

Figure 1(a) shows a schematic of the proposed microwave-microfluidic device, including a sensing resonator (resonator 1) and a heating resonator (resonator 2), fabricated on a glass substrate. The form of the experimental microfluidic system and the shape of droplets are also shown in figure 1(a). The designed microchannel is responsible for carrying the droplets, and the details of the microfluidic chip are shown in figure 1(b). The side view of our model exhibited the complex layers of the devices including the glass substrate, the resonators (only seen one in the side view), a passivation layer separating the resonators from the microchannel molded in polydimethylsiloxane (PDMS) and the dashed lines sketching the electrical field lines. A signal generator has been used to apply RF power producing heat, and a vector network analyzer (VNA) measures the microwave sensing results. When two resonators are placed close to each other, there will be interactions between their EM fields, and as a result of this mutual coupling between the two resonators, crosstalk occurs. This interference could seriously affect the sensing and detection results that influence the control and precision of the whole system since precise sensing is required to create reliable heat on the droplet. In the proposed design, the impact of high-power RF signal used to excite the heating resonator on the sensing resonator, which will significantly influence the detection results, is also one of the major concerns. A key factor determining the level of crosstalk is the physical distance between the two resonators, which must be studied in order to find an optimal length because too small a distance could cause significant crosstalk effects and too large a distance limits its multiplexing potential for a typical microfluidic device.

The key objective of this work is to numerically and experimentally investigate the impact of different design factors on the crosstalk between the two resonators that are integrated in a microfluidic device. The considered design factors include the distance between the two resonators (referred to as gap distance, d, in figure 2), resonator design, and microwave power. To focus on the crosstalk, the same design of the two resonators is considered. Numerical simulation in this work is served as a main tool to construct the chip model and investigate the crosstalk between the two resonators. ANSYS HFSS is employed to simulate different configurations and conditions with varying parameters, including the gap distance, the radius of two resonators, and the input power. Transmission parameters and scattering parameters are presented for crosstalk investigation. The justification of the assumptions in this work has been analyzed in detail previously [28]. Therefore, some major assumptions have been made as follows: (a) droplets are stationary on the top of resonators, which is considered such that droplet motion does not influence the electrical field; (b) the droplets are studied as directly contacting with the channel wall and the gutter region at the intersection of the cornets, and 3D droplet shapes are considered, and (c) the dielectric constants of the droplet and chip materials in the simulation are considered as constant to neglect their effect on the electrical field.

2.2. Designing microwave resonator-based structure

The numerical model is constructed in HFSS with two resonators illustrated in figure 2. A microfluidic system with two identical resonators is designed and simulated, and the design dimensions are also included in figure 2. The microwave signal is fed through the outer loop microstrip line, the ports connected to subminiature version A (SMA) connectors, and coaxial cables. The inner loop is the SRR with a small gap, which is the hotspot of the resonator for sensing application. It is designed in a spiral shape to confine microwave energy and maximize its interaction with the microchannel aligned with the gap area. As mentioned before, the purpose of this work is to investigate the crosstalk phenomena in the microfluidic chip with multiple resonators. The gap distance, the radius of the inner and outer loop, and the power of excitation are among the most critical parameters that affect the crosstalk between the two resonators in the system. Figure 2 illustrates the geometric parameters, including the gap distance (d), the radius of the resonators (R_{in}) and the radius of the ports (R_{out}).

Besides the microwave structure design, the boundary condition setup in HFSS is a necessary part of the

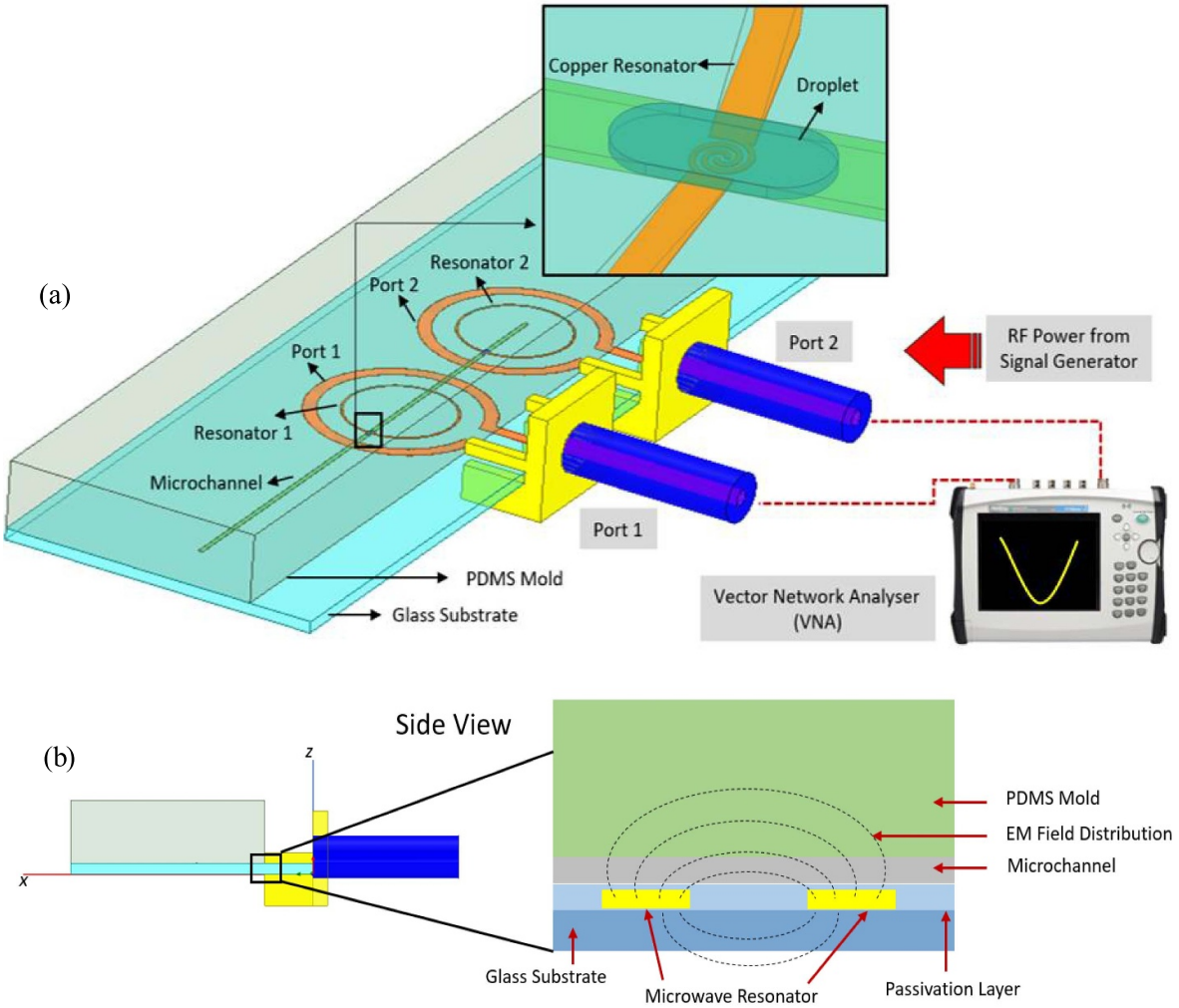

Figure 1. (a) Detailed schematic of the proposed microwave-microfluidic device for simultaneous heating and sensing and (b) side view of the microfluidic chip of model.

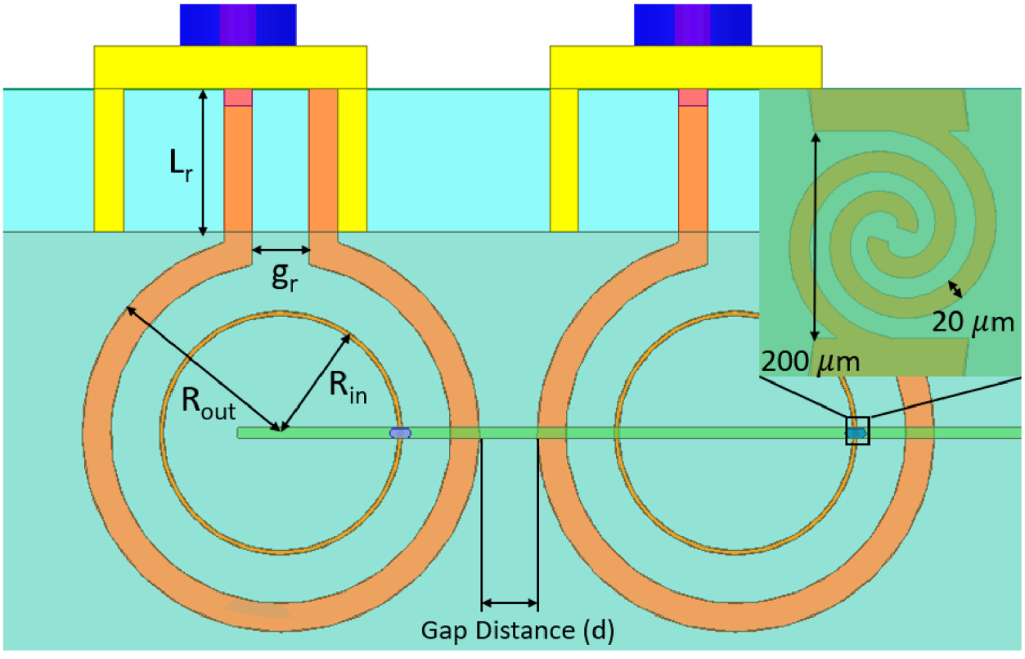

Figure 2. The main structure of the proposed design with the dimensions: $L_r = 5$ mm, $g_r = 2$ mm, $R_{\text{out}} = 6.95$ mm, $R_{\text{in}} = 4.25$ mm, $d = 2$ mm.

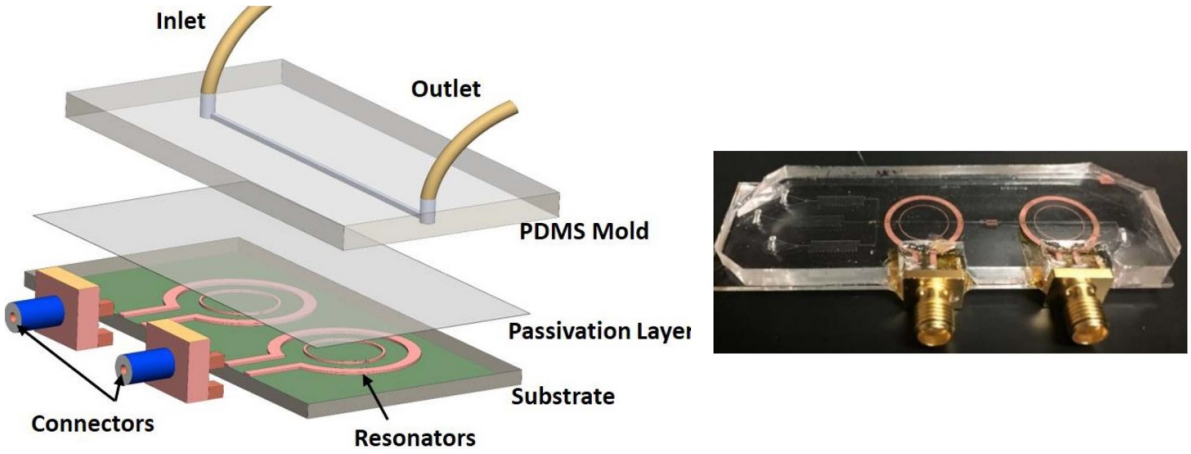

Figure 3. The schematic of components and fabricated microfluidic chip for validation.

numerical simulation since it defines the field behavior in the discontinuous boundaries. Applying the boundary conditions in HFSS helps control the characteristics of the planes' faces or interface between objects and reduces the complexity of the model. In addition to defining the boundary conditions, a specific solution setup is used for reliable and accurate results. More details are provided in the supplementary information.

2.3. Scattering parameter and sensing analysis

The behavior of the microwave resonator is characterized and evaluated by scattering parameters (S-parameters). In the proposed platform, a two-port network is considered due to the existence of two microwave resonators. S-parameter can help us analyze the power transfer and reflection between each port. The reflection coefficient, S11, is used to determine the change in material properties in the resonator region for sensing purposes. It is the ratio of reflected power to incident power for a given port. Transmission coefficient, S12, characterizes the ratio of the reflected power in port 1 over the incident power in port 2. In this study, the transmission coefficient is used to evaluate the crosstalk by analyzing the power transferred to port 1 relative to the input power at port 2.

The S12 response of the microwave sensor is dependent on the electrical characteristics of the ambient surrounding it. The main microwave circuit in the proposed design is SRR, and the initial resonance frequency of the resonator is related to its physical length (l) according to the following equation:

$$l = \frac{1}{2\sqrt{\varepsilon_{\text{eff}}}}\frac{c}{f_{\text{r}}} \tag{1}$$

where c is the speed of light (m s^{-1}), f_{r} is the resonance frequency (Hz), and ε_{eff} is the effective permittivity (F m^{-1}) of the resonator medium that is determined by the material surrounding the resonator [33]. The variation in ε_{eff} will affect the resonance frequency to shift up/down depending on the sample under test. Assuming the complex permittivity of the material under test over the resonator is a complex value:

$$\varepsilon = \varepsilon_r - j\varepsilon'' \tag{2}$$

where ε_{r} is the relative permittivity, which is a measure of how much energy from an external electric field is stored in a material. The imaginary part ε'' is called the loss factor and is a measure of dissipation or loss of a material in the presence of an external electric field. The presence of the material in the ambient around the resonator will act as the most effecting element to change ε_{eff}, making it suitable for sensing. On the other hand, the variation in ε'' will be reflected in amplitude variation and quality factor [16].

2.4. Experimental method

The fabrication of a microfluidic chip is based on soft lithography. The fabrication of microwave resonators relies on electroplating on a copper-coated glass slide (Cu134 from EMF Corporation), and more details can be found elsewhere [34]. The difference between the previously fabricated single resonator and the two resonators lies in the alignment of two resonators in a single glass slide, which requires the entire electroplating process to be more precise and careful. Microfluidic chips with two resonators that have a different gap distance are fabricated to validate the simulation results. After the electroplating procedure mentioned above, plasma treatment is carried out with a glass slide and a PDMS mold. The plasma treatment tightly follows bonding of the glass slide and PDMS mold under the microscope, and a marker in the glass slide is used to ensure that the two resonators are in the middle of the microchannel in the PDMS mold. The chip image and schematic are shown in figure 3. VNA (MS2028C, Anritsu) is used here to characterize resonator sensing performance and evaluate the crosstalk problem.

3. Results and discussion

3.1. The effect of gap distance on crosstalk

In this work, the gap distance is critical as it directly affects the coupling strength between the two resonators, a dominant factor for the determination of crosstalk. The smaller the gap distance is, the higher the interference they have on each other

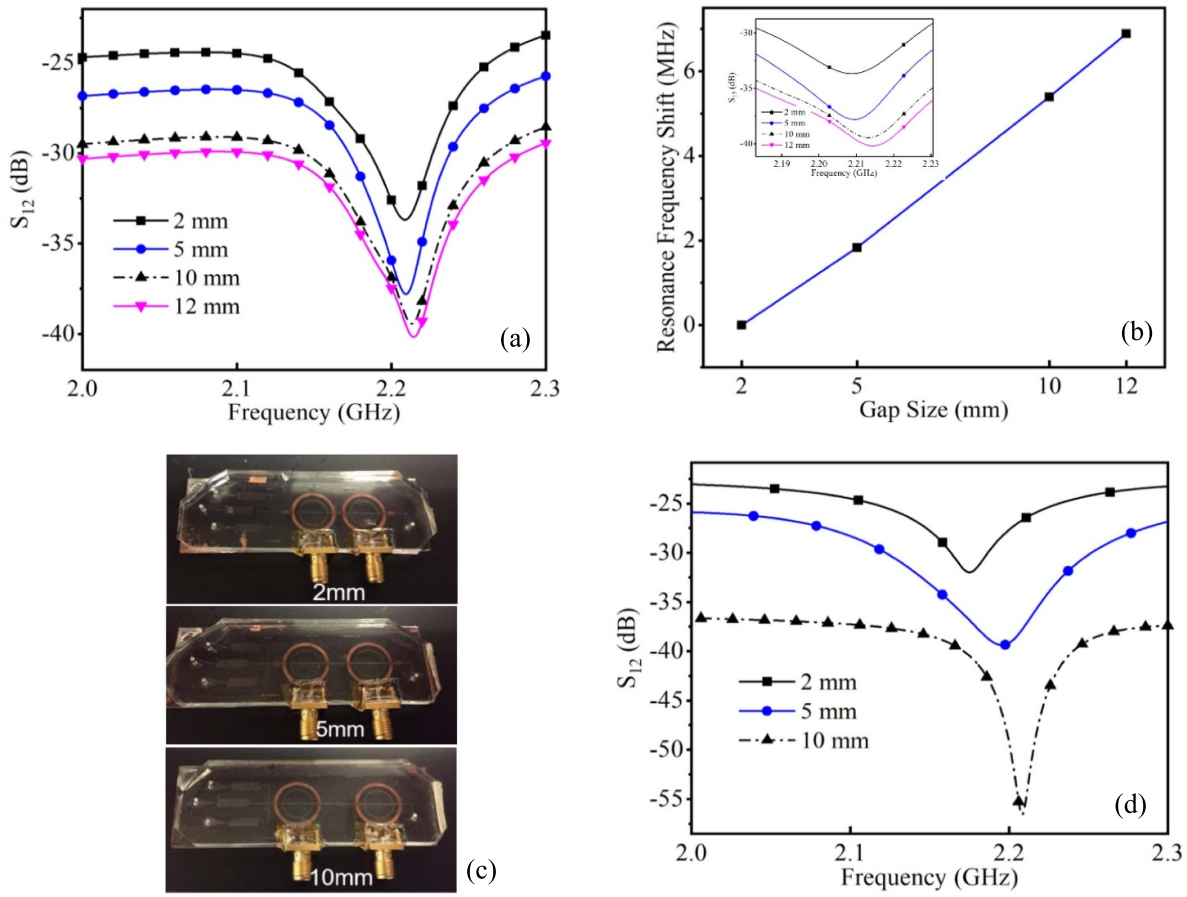

Figure 4. (a) Numerical simulation results for S12 while changing minimum gap size between the two resonators: 2 mm, 5 mm, 10 mm, and 12 mm, (b) frequency shift versus gap size as it changes from 2 mm to 12 mm, (c) fabricated device for different gap size values, and (d) measurement results for the S12 response $d = 2$ mm, 5 mm, and 10 mm.

in terms of performance. Also, crosstalk becomes a more significant issue for microfluidic applications due to their small devices, which adds a limitation to the location of the transmission lines. Therefore, it is necessary to find an optimal gap distance to prevent crosstalk while maximizing multiplexing potential. The gap distance in the numerical simulation is defined as the minimum distance between the two outer loops (d), which varies from 2 mm to 12 mm. The choice of 2 mm as the smallest gap distance is due to the fabrication limitations since enough space is required for the two SMA connectors being soldered. Considering the overall channel structure and microchip size and to avoid failure of the fabrication process, the upper limit for the gap distance is set as 12 mm. Figure 4(a) exhibits the simulation results for S12 parameter versus frequency for different gap distance values. Both the amplitude and resonance frequency variation of the S12 response are affected by the gap distance as shown in figure 4(a). The resonance frequency shift for the gap distance range is shown in figure 4(b). The results presented in figure 4 also highlight that the S12 response amplitude level increases as the gap distance decreases, which results from stronger coupling and more power transfer from port 1 to port 2. When the S12 goes lower in amplitude in the frequency range, it means less power is coupled between the two resonators, and less crosstalk would be the result. For example, when the gap distance increases from 2 mm to 5 mm, the S12 amplitude at the resonance frequency changes by 12.2%, and the change decreases to 4.3% from 5 mm to 10 mm and then 1.89% from 10 mm to 12 mm resulting from weak coupling in the range of 10–12 mm. Therefore, the 12 mm case is not tested in the experiments. The fabricated devices with $d = 2$ mm, 5 mm, and 10 mm are presented in figure 4(c) followed by the measurement results in figure 4(d). In figure 4(d), the transmission coefficient S12 shows a similar trend as the simulation results. When the gap distance increases, the S12 parameter decreases indicating that there is a reduction in the crosstalk. The S12 parameter of the 10 mm case has the smallest value among the three cases showing less coupling effect and presents the best performance to eliminate crosstalk. Although a similar trend is observed for the effects of the gap distance on the crosstalk, there are discrepancies in the S12 amplitude. This is mainly due to the imperfect experimental conditions, such as the imperfect connection of the SMA connector and the quality of the coaxial cable which could induce loss when being used for a long time.

As shown in figures 4(a) and (b), the resonance frequency is also impacted as the gap distance changes. A circuit model of the design is shown in figure 5(a) for further understanding by analysing the resonance frequency variation in the

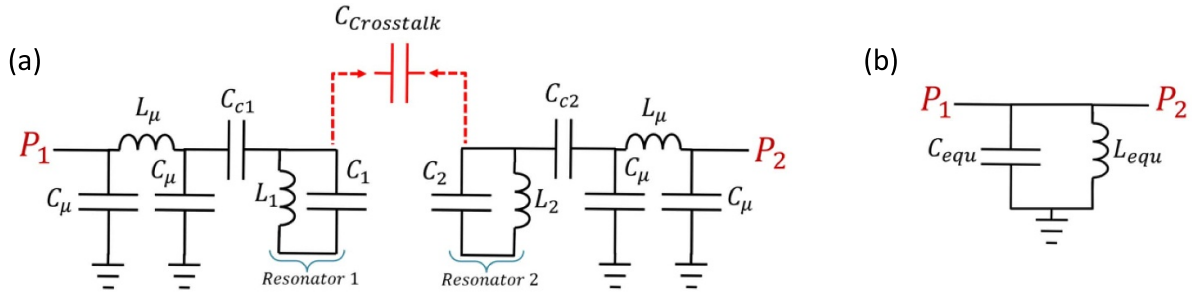

Figure 5. (a) A detailed and (b) an equivalent circuit model for the proposed dual-resonator structure with advanced design systems simulations.

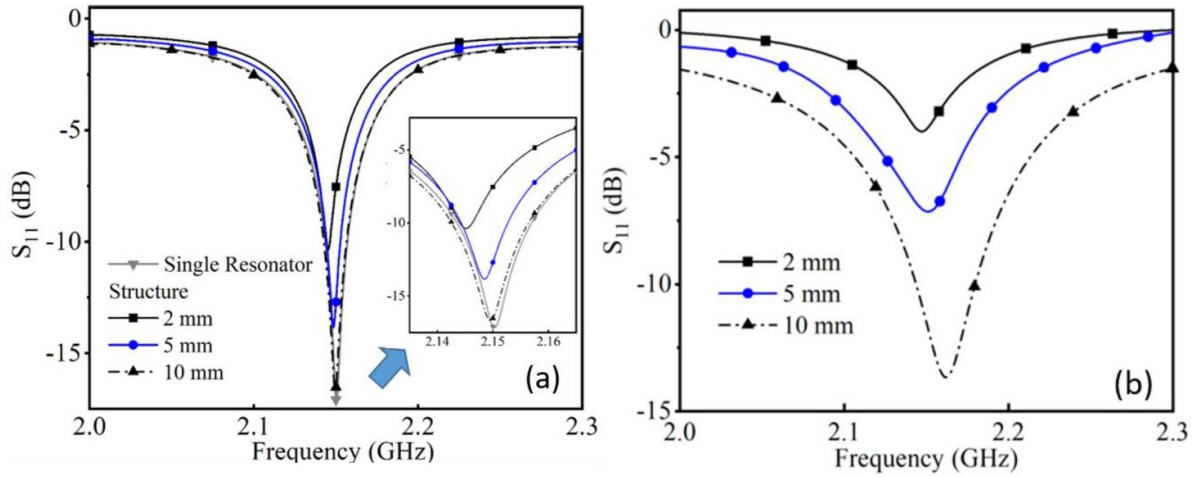

Figure 6. (a) Simulation and (b) measurement results of S11 for different gap distance values.

response by changing the gap distance. In figure 5(a), C_μ and L_μ describe the microstrip copper line of port 1 and port 2, which are coupled to the ideal (lossless) resonator with coupling capacitors C_{c1} and C_{c2}. The ideal resonator is modelled with a parallel inductor and capacitor, $C_1 - L_1$ for the resonator coupled to port 1 and $C_2 - L_2$ for the resonator coupled to port 2 [19, 35]. Another considerable effect is created by the presence of $C_{\text{Crosstalk}}$ since the closeness between the two ports/resonators forms an unwanted capacitor which is a circuit definition for the crosstalk. By increasing the distance, the coupling capacitance in the gap, $C_{\text{Crosstalk}}$, becomes a smaller value, and as a result of that, the equivalent capacitance of the circuit model (C_{equ}) will be impacted (figure 5(b)). Referring to the relation between the resonance frequency (f_r) and the equivalent capacitance and inductance of the circuit model ($f_r = \frac{1}{2\pi\sqrt{L_{\text{equ}} C_{\text{equ}}}}$) and considering the fact that C_{equ} and $C_{\text{Crosstalk}}$ are directly correlated, the resonance frequency with be impacted by the variation of the gap distance. A larger gap results in a smaller value of $C_{\text{Crosstalk}}$ and reduces the equivalent capacitance of the whole two-port circuit and this creates an upshift in frequency, which is verified in simulations and measurements.

Figure 6(a) describes the simulation for S11 while the resonator, coupled with port 2, performs microwave heating. Port 2 is connected to a power input of 26 dBm, a standard power level used in microfluidic heating experiments [34], and port 1 is connected to the VNA to monitor variation around the coupled resonator, which is a microwave sensing device. To evaluate the effect of crosstalk initiated from the strong microwave signal in the heating resonator on sensing performance, S11 of a single resonator structure is used as the reference which has no crosstalk effect. It can be seen that the S11 signal in the dual resonator structure is approaching to that of the one resonator case when the gap distance increases, showing the reduced crosstalk. The maximum crosstalk occurs for the 2 mm gap distance case. As shown in figure 6(a), the resonance frequency in the S11 response moves to upper frequencies as the gap distance increases, which is also the result of decreasing $C_{\text{Crosstalk}}$ and C_{equ}. Figure 6(b) shows the S11 measurement results from the fabricated device while the second resonator is used for heat production. It suggests that as the distance increases from 2 mm to 10 mm, the crosstalk is decreasing. The experimental results and the numerical simulation results confirm that a 10 mm interval for two resonators is an optimal distance to minimize crosstalk. The difference between numerical simulation and experimental measurement results is mainly due to the imperfect conditions in real experiments such as imperfect SMA connections, which are usually ideal in numerical simulation. It is noted that this study focuses on evaluating the cross talk, and thus, although

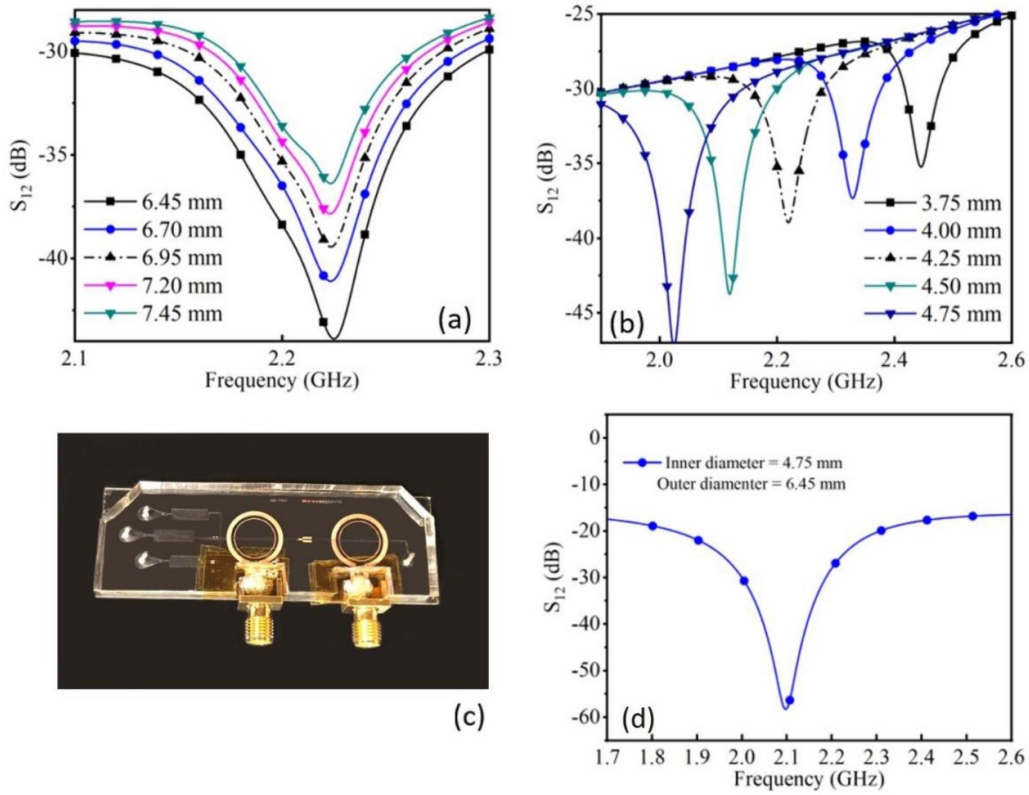

Figure 7. (a) Numerical simulation results for different outer loops, (b) numerical simulation results for different inner loops, and (c) a resonator design with the smallest outer loop (i.e. 6.45 mm) and the largest inner loop (i.e. 4.75 mm) (d) experimental measurement results for the optimal case.

the power is supplied to the heating resonator, the resulted temperature increase is not characterized. Demonstration of simultaneous sensing and heating with the findings of the minimized crosstalk justifies an extensive project by itself.

3.2. The effect of resonator radius on crosstalk

Based on the numerical and experimental results presented in figures 4 and 6, 10 mm is the optimal gap distance for minimizing the crosstalk, which can be further reduced by varying the design of the resonators such as the radius of the resonators, R_{in}, and the ports, R_{out}. The outer loop in the resonator structure is designed to be excited with microwave signal and transfer the signal to the resonator, which is designed as the inner loop, through EM coupling. In regular cases, R_{in} and R_{out} are set as 4.25 mm and 6.95 mm respectively which have been varied by $\pm$0.5 mm with an increment of 0.25 mm. Figure 7(a) shows the effect of the outer loop radius on the S12 parameter while keeping the inner loop radius being 4.25 mm. It can be observed that the amplitude of the S12 response drops as the outer diameter decreases, which indicates that a smaller outer loop provides a stronger coupling between the excitation port (outer loop) and the resonator (inner loop) and thus smaller crosstalk. In these cases, the resonance frequency stays consistent because the effect of the outer loop radius variation on C_{equ} and L_{equ} is negligible. As shown in figure 7(b), the amplitude of the S12 parameter decreases with increasing inner loop radius, implying reduced crosstalk because a larger inner loop allows a strong coupling with the excitation outer loop. The resonance frequency of the S12 response reduces with increasing inner loop radius because the resonator's total length is reversely correlated as mentioned in equation (1). From these two studies, it can be concluded that the resonator design plays an important role in crosstalk and reducing the distance between the two loops (either increasing the radius of the inner loop or decreasing outer loop radius) can help to alleviate crosstalk between two adjacent resonators. To validate this finding, a resonator design with the smallest outer loop (i.e. 6.45 mm) and the largest inner loop (i.e. 4.75 mm) shown in figure 7(c) is fabricated and experimentally tested as presented in figure 7(d). Compared with the original case in figure 4(d), there is a drop in the S12 value indicating a reduction of the crosstalk.

3.3. The effect of signal generator power on crosstalk

A broader definition of crosstalk can be understood as any undesired signal that interferes with the target signal. The signal strength also affects crosstalk, besides manipulating the structure and gap distance of the two resonators. The heating resonator receives signal with high power and the high power could cause an undesired signal in the sensing resonator. As a result, it is necessary to investigate the impact

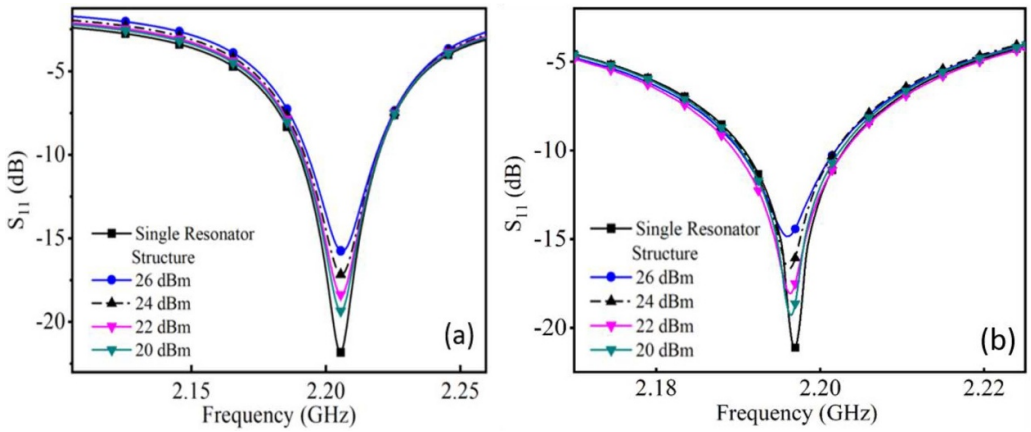

Figure 8. (a) Simulation and (b) measurement results for investigating power influence on crosstalk.

of the power level received in the heating resonator on the sensing resonator coupled to port 1. Changing the input power level connected to port 2 for heating purpose will change the transmitted power from port 1 to port 2, and as a result of it the reflective power characterized by S11 which is an indicator of crosstalk. Therefore, S11 is used to evaluate the effect of microwave power on crosstalk. Figure 8(a) depicts the numerical results of the power effect on crosstalk. The input power varies from 26 dBm to 20 dBm. The S11 signal with different input power is compared with one resonator case, which is considered no crosstalk. The corresponding experiments are performed, and the results are presented in figure 8(b), which agree with the numerical results reasonably well. As the input power value decreases, S11 signal gets closer to the no crosstalk case, meaning that the crosstalk is reduced. Therefore, minimized input power is desired to prevent crosstalk if it is high enough to produce the required heating for a specific application.

4. Conclusions

In this study, we numerically and experimentally investigated the crosstalk between two adjacent resonators integrated in a microfluidic chip and the effect of crosstalk on the sensing performance of the design. In particular, we aimed to overcome the crosstalk phenomena by investigating the influence of parameters, including the distance between the two resonators, the radius of the excitation and resonator loops, and the input power. After the calculation of numerical simulation and experimental validation, an optimal distance of 10 mm between the two resonators is confirmed with less crosstalk inference and can be used for the next step experiments. The resonator design plays an important role in crosstalk and it is found that increasing the inner loop radius or decreasing the outer loop radius can alleviate the crosstalk between two adjacent resonators. Lower input power if applicable is desired to reduce crosstalk. This study gives an understanding about the crosstalk between two resonators in a typical microfluidic chip and offer strategies to minimize the crosstalk influence for double resonators.

Data availability statement

The data that support the findings of this study are available upon reasonable request from the authors.

Acknowledgments

The authors would like to acknowledge the support from the Canadian Research Chair Program, Natural Sciences and Engineering Research Council of Canada (RGPIN-2018-04151) and Ontario Research Fund (ORF-RE09-016) through Grants to Dr Carolyn Ren.

ORCID iDs

Zahra Abbasi https://orcid.org/0000-0002-7422-5056
Carolyn L Ren https://orcid.org/0000-0002-9249-7397

References

[1] Abgrall P and Gue A 2007 Lab-on-chip technologies: making a microfluidic network and coupling it into a complete microsystem—a review *J. Micromech. Microeng.* **17** R15
[2] Guo M T, Rotem A, Heyman J A and Weitz D A 2012 Droplet microfluidics for high-throughput biological assays *Lab Chip* **12** 2146–55
[3] Zeng W, Jacobi I, Li S and Stone H A 2015 Variation in polydispersity in pump- and pressure-driven micro-droplet generators *J. Micromech. Microeng.* **25** 115015
[4] Markey A L, Mohr S and Day P J 2010 High-throughput droplet PCR *Methods* **50** 277–81
[5] Ba E, Won S, Kim D J and Kim J G 2015 Development and analysis of a capacitive touch sensor using a liquid metal droplet *J. Micromech. Microeng.* **25** 095015
[6] Chin C D, Linder V and Sia S K 2012 Commercialization of microfluidic point-of-care diagnostic devices *Lab Chip* **12** 2118–34
[7] Shamsi M H and Chen S 2017 Biosensors-on-chip: a topical review *J. Micromech. Microeng.* **27** 083001–17
[8] Chen X and Ren C L 2017 A microfluidic chip integrated with droplet generation, pairing, trapping, merging, mixing and releasing *RSC Adv.* **7** 16738–50

[9] Li H, Men D, Sun Y, Zhang T, Hang L, Liu D, Li C, Cai W and Li Y 2017 Optical sensing properties of Au nanoparticles/hydrogel composite microbeads using droplet microfluidics *Nanotechnology* **28** 40
[10] Ullah N, Mansha M, Khan I and Qurashi A 2018 Nanomaterial-based optical chemical sensors for the detection of heavy metals in water: recent advances and challenges *TrAC Trends Anal. Chem.* **100** 155–66
[11] Hadwen B, Broder G R, Morganti D, Jacobs A, Brown C, Hector J R, Kubota Y and Morgan H 2012 Programmable large area digital microfluidic array with integrated droplet sensing for bioassays *Lab Chip* **12** 3305–13
[12] Niu X, Zhang M, Peng S, Wen W and Sheng P 2007 Real-time detection, control, and sorting of microfluidic droplets *Biomicrofluidics* **1** 44101
[13] Srivastava N and Burns M A 2006 Electronic drop sensing in microfluidic devices: automated operation of a nanoliter viscometer *Lab Chip* **6** 744–51
[14] Yesiloz G, Boybay M S and Ren C L 2015 Label-free high-throughput detection and content sensing of individual droplets in microfluidic systems *Lab Chip* **15** 4008–19
[15] Abdolrazzaghi M, Daneshmand M and Iyer A K 2017 Strongly enhanced sensitivity in planar microwave sensors based on metamaterial coupling *IEEE Trans. Microw. Theory Tech.* **66** 1843–55
[16] Abbasi Z, Baghelani M, Nosrati M, Sanati-Nezhad A and Daneshmand M 2019 Real-time non-contact integrated chipless RF sensor for disposable microfluidic applications *IEEE J. Electromagn. RF Microw. Med. Biol.* **4** 171–8
[17] Velez P, Munoz-Enano J, Grenier K, Mata-Contreras J, Dubuc D and Martin F 2018 Split ring resonator (SRR) based microwave fluidic sensors for electrolyte concentration measurements *IEEE Sens. J.* **19** 2562–9
[18] Abduljabar A A 2016 Compact microwave microfluidic sensors and applicator Cardiff University
[19] Abbasi Z, Shariaty P, Nosrati M, Hashisho Z and Daneshmand M 2019 Dual-band microwave circuits for selective binary gas sensing system *IEEE Trans. Microw. Theory Tech.* **67** 4206–19
[20] Abbasi Z, Zarifi M H, Shariaty P, Hashisho Z and Daneshmand M 2017 Flexible coupled microwave ring resonators for contactless microbead assisted volatile organic compound detection *2017 IEEE MTT-S Int. Microwave Symp. (IMS)* (https://doi.org/10.1109/MWSYM.2017.8058827)
[21] Baghelani M, Abbasi Z, Daneshmand M and Light P E 2020 Non-invasive continuous-time glucose monitoring system using a chipless printable sensor based on split ring microwave resonators *Sci. Rep.* **10** 12980
[22] Hamzah H, Lees J and Porch A 2018 Split ring resonator with optimised sensitivity for microfluidic sensing *Sens. Actuators* A **276** 1–10
[23] Muoz-Enano J, Vélez P, Gil. M and Martín F 2020 Planar microwave resonant sensors: a review and recent developments *Appl. Sci.* **10** 2615
[24] Turgul V and Kale I 2018 Permittivity extraction of glucose solutions through artificial neural networks and non-invasive microwave glucose sensing *Sens. Actuators* A **277** 65–72
[25] Fang W and Burns M A 2009 Performance of nanoliter-sized droplet-based microfluidic PCR *Biomed. Microdevices* **11** 1071
[26] Murshed S and Castro C 2014 *Nanofluids: Synthesis, Properties and Applications* Nanotechnology Science and Technology (Nova) p 296 BISAC: TEC027000
[27] Miralles V, Huerre A, Malloggi F and Jullien M C 2013 A review of heating and temperature control in microfluidic systems: techniques and applications *Diagnostics* **3** 33–67
[28] Cui W, Yesiloz G and Ren C L 2020 Numerical analysis on droplet mixing induced by microwave heating: decoupling of influencing physical properties *Chem. Eng. Sci.* **224** 115791
[29] Issadore D, Humphry K J, Brown K A, Sandberg L, Weitz D A and Westervelt R M 2009 Microwave dielectric heating of drops in microfluidic devices *Lab Chip* **9** 1701–6
[30] Hamzah H 2017 Microwave microfluidic resonant sensors and applicators Cardiff University
[31] Boybay M S, Jiao A, Glawdel T and Ren C L 2013 Microwave sensing and heating of individual droplets in microfluidic devices *Lab Chip* **13** 3840–6
[32] Cui W, Yesiloz G and Ren C L 2020 Microwave heating induced on-demand droplet generation in microfluidic systems *Anal. Chem.* **93** 1266–70
[33] Lee H-J, Hyun K-A and Jung H-I 2014 A high-Q resonator using biocompatible materials at microwave frequencies *Appl. Phys. Lett.* **104** 023509
[34] Yesiloz G, Boybay M S and Ren C L 2017 Effective thermo-capillary mixing in droplet microfluidics integrated with a microwave heater *Anal. Chem.* **89** 1978–84
[35] Nosrati M and Daneshmand M 2017 Substrate integrated waveguide L-shaped iris for realization of transmission zero and evanescent-mode pole *IEEE Trans. Microw. Theory Tech.* **65** 2310–20